

# Development of a Low-Cost Machine Vision System and Its Application on Inspection Processes

Yu-Chieh Chen and Yin-Tien Wang\*

*Department of Mechanical and Electro-Mechanical Engineering, Tamkang University,  
Tamsui, Taiwan 251, R.O.C.*

## Abstract

A low-cost machine vision system with hardware capabilities of image processing is developed in this research. Several image process algorithms are designed for the developed vision system, namely, image quality selection, image recovery and resize, and image segmentation. All of these mathematical algorithms are programmed and implemented in a microchip using SOPC design tools. Furthermore, the developed machine vision system is utilized in the automatic inspection process to detect the position of a compact disk in CD/DVD duplicators. In the process, the inspection algorithm is based on the two-value image provided by the machine vision system. In the near future, an attempt will be made to apply this vision system to CD/DVD label printers. Meanwhile, the integrated system has the potential usage on many low price automation products.

**Key Words:** CMOS Vision, Visual Inspection, Machine Vision System, System on a Programmable Chip

## 1. Introduction

CMOS vision modules had been developed for years and widely used in optical mouse, webcam, and photo device in a cell phone. Due to the huge amount of demand, the cost and the physical dimension of a CMOS vision module has dramatically reduced, however, the resolution of the image taken by the CMOS vision has been increased. In this research, a methodology is proposed to utilize these CMOS sensor modules in automatic visual inspection devices and to replace the conventional and high-cost sensors based on ultrasonics, laser, or optical encoder [1,2].

The usages of vision in industrial inspection instrumentation are quite different from those in human vision appliances. Human vision is sensitive to the contrast of color hue, the difference of lightness, and the edges between the object and environment, but is insensitive to the saturation and brightness of similar color hues in an image [3]. Therefore, vision systems in human appli-

ances utilize techniques, such as white balancing and brightness control, to repair an image and provide a good-looking image to human vision systems [4]. On the other hand, in an industrial inspection process, the machine vision system should provide a real and original image rather than a processed image [1,2]. In this research, several images are taken at different sampling frequencies, and then a selection procedure is performed to abandon the images with noise and to provide an image of original.

Applications of the developed vision system on an automatic inspection process will be investigated in this research. An attempt will be made to automatically detect the position of compact disk in an auto duplicator, and ensure the disk is precisely picked out from or loaded into the duplicator. The space is limited inside the duplicator for installation of the vision system, hence a small-size CMOS vision module is chosen in this case.

Several image process procedures will applied to the acquired image, including image restoration, image resize, and image segmentation [5], however these processes should not destroy the original of the image. All of

---

\*Corresponding author. E-mail: ytwang@mail.tku.edu.tw

the image process algorithms will be developed and implemented on a single-chip. We will make use of the SOPC design tools to integrate the hardware circuits and image process algorithms on a FPGA chip. The integrated system with CMOS vision sensors has the potential usage on many low price automation products.

## 2. Image Processing

Several procedures for digital image processing are needed for the developed visual inspection system, including image quality selection, image restoration, image resize, and image segmentation. First, several images are taken by the CMOS vision at different frequencies, and a procedure for image selection is performed according to an image quality index. Second, the image distortion due to the usage of CMOS visions must be corrected by an image recovery procedure. Furthermore, the restored image is enlarged in order to increase the resolution of inspection. Finally, an image segmentation procedure is applied to determine the object of interest in the image.

### 2.1 Image Selection

In order to select the best image quality, several sub-image blocks are analyzed instead of a full image that contains  $n \times n$  pixels. Choose an image unit that contains  $l \times l$  numbers of pixels, and define  $GL$  (Gray Level) as the average gray level in an image unit:

$$GL = \frac{1}{l^2} \sum_{i=1}^l \sum_{j=1}^l O(i, j) \quad (1)$$

where divided by  $l^2$  is to ensure that the value of  $GL$  is converged;  $O(i, j)$  is the gray level of each pixel in the chosen image unit. We further define  $AGL$  (Average Gray Level) for the full image:

$$AGL = \frac{1}{n^2} \sum_{i=1}^n \sum_{j=1}^n GL(i, j) \quad (2)$$

where  $n^2$  is the coefficient to ensure the value of  $AGL$  converged. Totally  $m \times m$  numbers of image units are gathered to form a sub-image block for image analyzing. If there are noise pixels in a sub-image block, there must have some image units containing unusual  $GL$  values comparing to the value  $AGL$ . Define  $d_1$  to be the

difference between the smallest  $GL$  and the  $AGL$ , and  $d_2$  to be the difference between the largest  $GL$  and the  $AGL$  as in Figures 1 and 2. If the values of  $d_1$  and  $d_2$  are larger than the expected values, as seen in Figure 1, the image is noise involved. On the contrary, as shown in Figure 2, the image has reasonable good quality. A structural degree ( $SD$ ) is defined to referee whether an image is noise involved or not,

$$SD = |[\max(GL) - AGL] - [AGL - \min(GL)]| \quad (3)$$

A sub-image block is noise involved when its  $SD$  index is larger than expected. The  $SD$  index is utilized in this research to filter out the noise involved image blocks. Among the noise-free image blocks, one with best quality is selected according to the value of background luminance ( $BL$ ) [3]:

$$BL = \max(GL) - \min(GL) \quad (4)$$

An image has a better quality than the others, if its  $BL$  value is larger than that of the others.

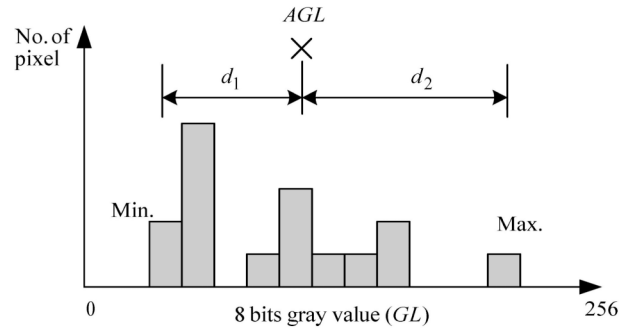


Figure 1. Noise involved image.

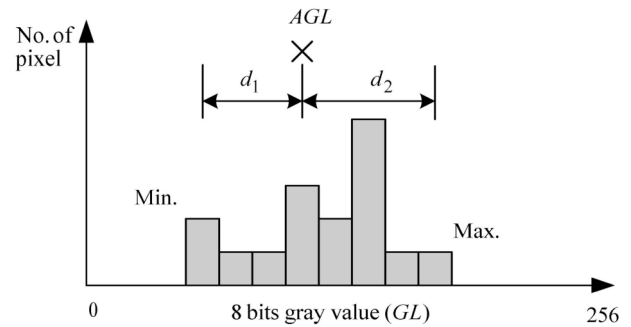


Figure 2. Good quality image.

## 2.2 Image Recovery

A low-cost CMOS sensor is always equipped with a universal lens, and applied to observe objects in a large range of distance without tuning the focus of the lens. However, the usage of universal lens will induce the problem of image distortion. As shown in Figure 3, the grids in the center of the picture are enlarged, while those in the corners are squeezed. The distortion ratio is a non-linear function of the radius from the center of the picture, as shown in Figure 4. A polynomial equation is applied to correct the pixel positions in the selected image,

$$R = a_0 + a_1 r + a_2 r^2 + \dots + a_n r^n$$

where  $r$  is the radius from the center of the image to the

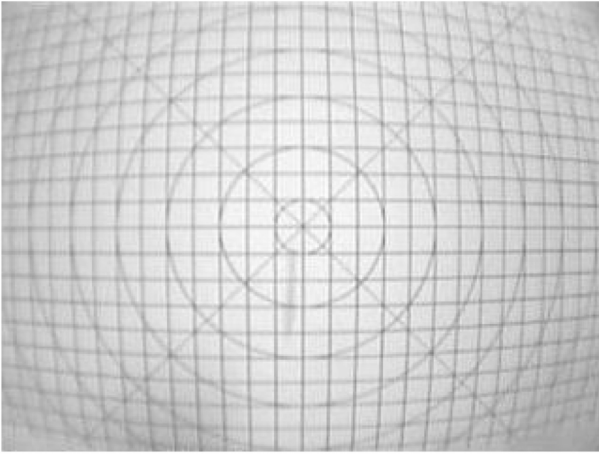


Figure 3. Distorted image

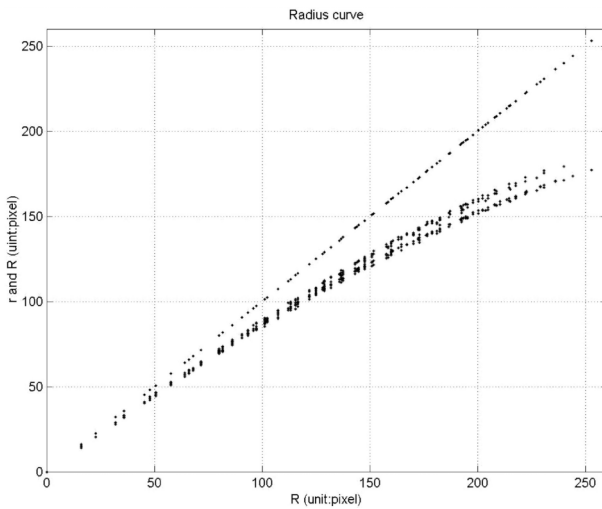


Figure 4. Positions of the grids in the distorted image

position of the pixel;  $R$  is the corrected radius; The coefficients  $a_0, \dots, a_n$  can be determined by using a curve-fitting method [6].

Another image problem is caused by perspective project of lens. When two points locate at different heights from the sensor, they could not be found the correct position by the same perspective transformation matrix, as shown in Figure 5. An offset is compensated for the height difference in the transformation matrix to get the correct pixel position.

## 2.3 Image Resize

The restored image is then resized by using the bilinear interpolation method [4,5–8] to increase the resolution of each pixel in the image. In this paper, gray level image are utilized, and the values of the gray level is defined as the following equation:

$$O(x, y) = i(x, y) \times r(x, y)$$

where  $i(x, y)$  is a function proportional to energy of the light source, and  $0 \leq i(x, y) < \infty$ ;  $r(x, y)$  is the light reflection ratio of the object which is a characteristic of the object, and  $0 \leq r(x, y) \leq 1$ . In Figure 6, the sized of the image is zoomed in to be four times larger than that of the original image. The pixels of the original image are uniformly dispersed into a new image. The blank pixels,  $P(x', y')$ , in the new image are filled by new pixel values  $v(x', y')$ ,

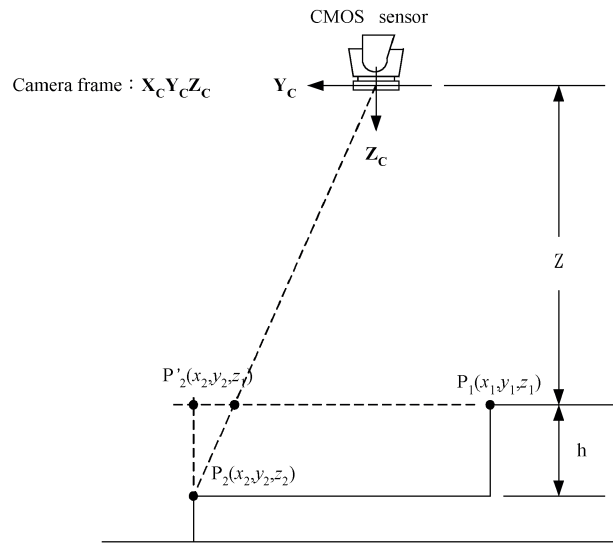


Figure 5. Objects at different heights

O(0,0)		O(1,0)		O(2,0)		O(3,0)	
O(0,1)		O(1,1)	P(1,0)	O(2,1)		O(3,1)	
		P(0,-1)	P(1,-1)				
O(0,2)		O(1,2)		O(2,2)		O(3,2)	
O(0,3)		O(1,3)		O(2,3)		O(3,3)	

Figure 6. Bilinear interpolation method

$$v(x', y') = ax' + by' + cx'y' + d \quad (5)$$

The coefficients  $a, b, c, d$  are determined by using a curve-fitting method [7].

## 2.4 Image Segmentation

The enlarged image is then segmented by using a threshold method [5,7] in order to distinguish the pixels between the object and the background. Before the image segmentation, the edge of the object in the image is enhanced to avoid the possibility of pixel discontinuity. Sobel masking method [9,10] is utilized to search the edge of an object and a discontinuous pixel value inside the object will be replaced by the pixel value of the object. The Sobel mask is shown in Figure 7.

In the image segmentation procedure, the pixels represent the object is separated from those pixels represent the background by using a threshold value, as shown in Figure 8. In this research, an algorithm is proposed to

-1	-2	-1	-1	0	1
0	0	0	-2	0	2
1	2	1	-1	0	1

(a) (b)

Figure 7. Sobel mask (a) x direction mask, (b) y direction mask

automatically select a threshold value  $T$ :

- Estimate an initial threshold value  $T$  and define a stopping index  $\Delta T_0$ ;
- Use the value  $T$  to separate the pixels of the image into two groups:  $G_1$  contains the pixels  $O(x, y) > T$ , and  $G_2$  contains the pixels  $O(x, y) \leq T$ ;
- Determine the average values of gray level of  $G_1$  and  $G_2$  as  $\mu_1$  and  $\mu_2$ ;
- Calculate a new threshold value by

$$T' = \frac{1}{2}(\mu_1 + \mu_2)$$

And find the difference between these threshold values by

$$\Delta T = |T' - T|$$

- Repeat steps b to d until the value of  $\Delta T$  is smaller than the stopping index  $\Delta T_0$  defined in step a.

## 3. Machine Vision System

The developed machine vision system consists of an ET21X110A CMOS vision [11] and a Stratix EP1S10 FPGA chip [12]. The vision module, as shown in Figure 9, provides an image in analog and/or digital format with a resolution of  $32 \times 32$  pixels. Function block of the sensor is sketched as Figure 10. The FPGA chip is planned and possessed the capabilities to generate sampling frequencies, perform image processing, and communicate with the CMOS vision and personal computer, as shown in Figure 11. Note that the image processing algorithms are implemented using a Nios CPU, which is design by using the SOPC design tools Quartus II by Altera [12].

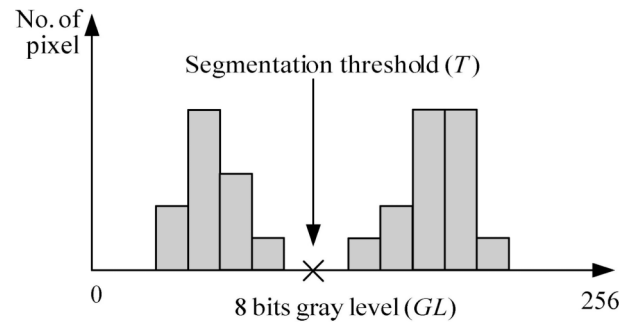


Figure 8. Threshold value

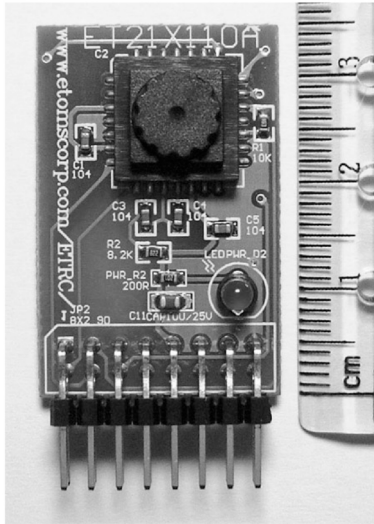


Figure 9. ET21X110A CMOS sensor module

Function blocks of the digital logic circuits shown in Figure 12 are designed in the FPGA to generate sampling frequencies for image acquisition.

#### 4. Application

As an example of application, the CMOS vision module is utilized to detect the center of a compact disk in a CD/DVD duplicator. First, the acquired image is divided into 16 sub-image blocks, as shown in Figure 13(a), and the

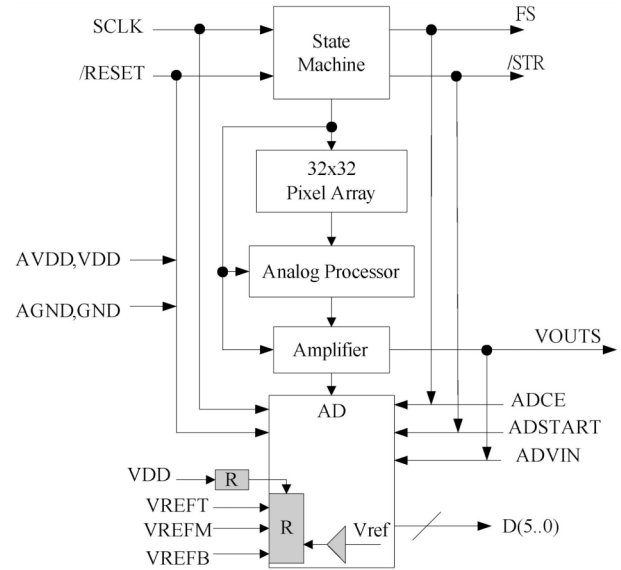


Figure 10. Function blocks of ET21X110A

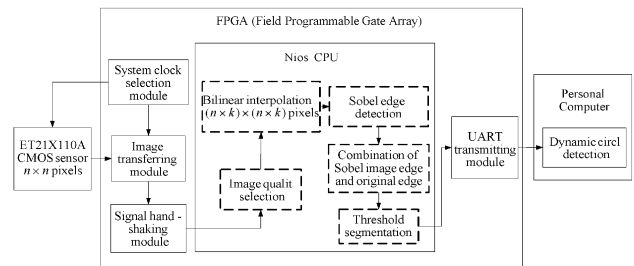


Figure 11. Function block of the programmed FPGA

#### ET21x110A System Module

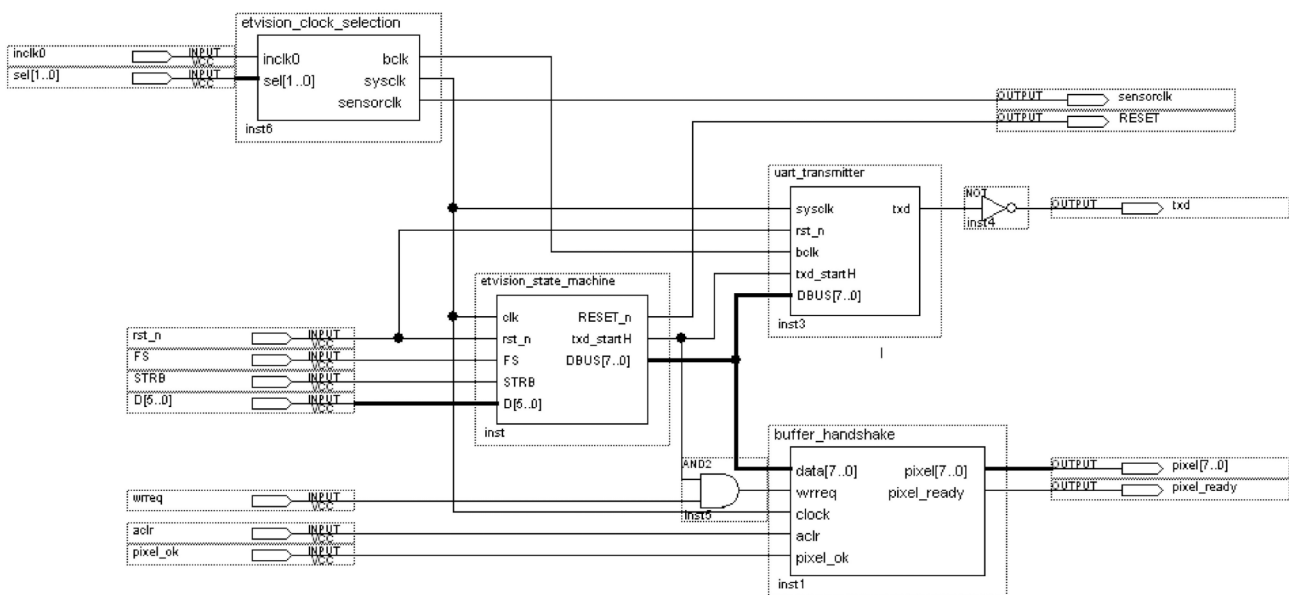
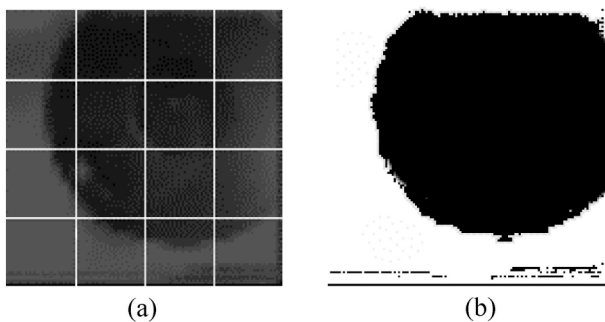


Figure 12. Function blocks of the FPGA digital logic circuits

blocks with high  $SD$  values are filtered out because of involution of noise. Second, the sub-image blocks with high  $BL$  values are selected to form a full image. Third, the selected image is recovered from distortion. Afterward the processes of resize and edge-detected are applied on the image. Finally, the contour image of the CD is determined by image segmentation, as shown in Figure 13(b). The center of the CD can be found by further usage of a weighted method. Figure 14 depicts the whole image processing procedure.

#### 4. Conclusion

A machine vision system with hardware capabilities



**Figure 13.** (a) A full image is divided into 16 sub-image blocks, (b) the image after use threshold method

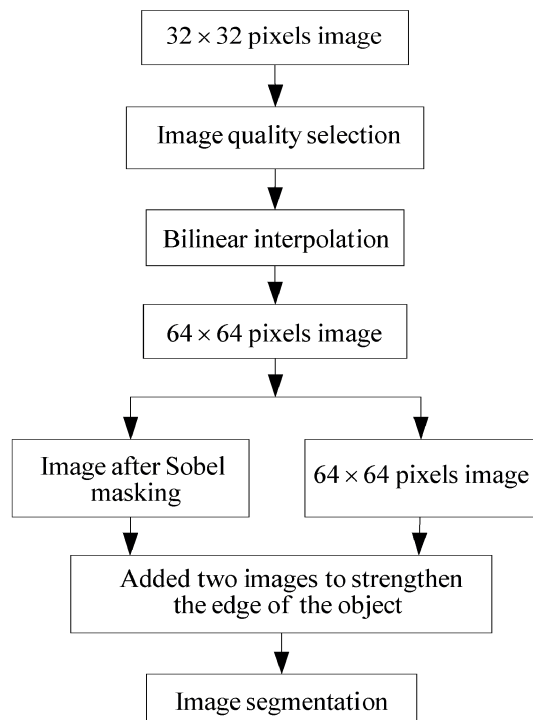


**Figure 14.** Image processing procedure

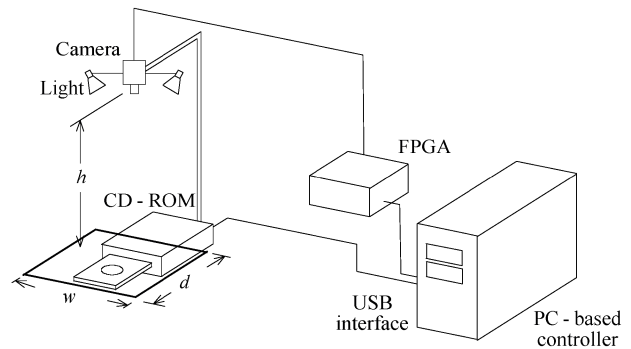


**Figure 15.** CD/DVD duplicator inspection setup

of image processing is developed using a low-cost CMOS vision in the paper and applied in an automatic inspection process to detect the position of a compact disk for CD/DVD duplicators. Several image process algorithms are designed for the developed vision system. All of these mathematical algorithms are implemented in a FPGA chip using the SOPC design tools.

Due to the advantages of low price and small dimension, the developed vision system with CMOS module has the potential usage on many automation products for the purposes of inspection or servoing control. However, more research efforts must be done on hardware implementation of image processing and increase of vision resolution.

#### Acknowledgements

This work was supported by the National Science Council in Taiwan under grant no. NSC93-2622-E-032-003-CC3.

#### References

- [1] Pai, A. L. and Lee, K., "Automated Visual Inspection of Aircraft Engine Combustor Assemblies," *Proceedings of IEEE International Conference on Robotics and Automation*, pp. 1919–1924 (1986).
- [2] Porter, G. B., Cipolla, T. M. and Mundy, J. L., "Automatic Visual Inspection of Blind Holes in Metal Surfaces," *Proceedings of IEEE Conference on Pattern Recognition and Image Processing*, pp. 83–86 (1979).
- [3] Mannos, J. and Sakrison, D., "The effects of a visual fidelity criterion of the encoding of images," *IEEE Transactions on Information Theory*, Vol. 20, pp. 525–536 (1974).



- [4] Pu, H. C., Liang, S. F. and Lin, C. T., "A HVS-Directed Neural-Network-Based Image Resolution Enhancement Scheme for Image Resizing," *Department of Electrical and Control Engineering, National Chiao-Tung University, Taiwan*, (2004).
- [5] Gonzalez, R. C. and Woods, R. E., *Digital Image Processing*, Prentice Hall, (2002).
- [6] Yu, W. H. W. and Huang, U. C., "An Efficient Geometric Curve Fitting Technique," *TENCON, Fourth IEEE Region 10 International Conference*, pp. 960–963 (1989).
- [7] Cheriet, M., Said, J. N. and Suen, C. Y., "A Recursive Thresholding Technique for Image Segmentation," *IEEE Transactions on Image Processing*, Vol. 7, pp. 918–921 (1998).
- [8] Unser, M., Aldroubi, A. and Eden, M., "Enlargement or Reduction of Digital Images with Minimum Loss of Information," *IEEE Transactions on Image Processing*, Vol. 4, pp. 247–258 (1995).
- [9] Sobel, I. E., *Camera Models and Machine Perception*, Ph.D. Thesis, Department of Electrical Engineering, Stanford University (1970).
- [10] Jensen, K. and Anastassiou, D., "Subpixel Edge Localization and the Interpolation of Still Image," *IEEE Transactions on Image Processing*, Vol. 4, pp. 285–295 (1995).
- [11] Etoms, *ET21X110A User's manual*, Etoms Inc. (2004).
- [12] Altera, *Stratix EP1S10 User's manual*, Altera Inc., <http://www.altera.com>.

**Manuscript Received: Jun. 30, 2007**

**Accepted: Jul. 24, 2008**